8. DEVELOPMENT OF ACTIVE SEPARATION CONTROL FEEDBACK SYSTEM

The vortex generator jet method has been studied since the first examination in the 1950's. In recent years, for the vortex generator jet method the effects of various parameters and longitudinal vortices on separation control begun to be understood gradually. However, any applications of vortex generator jets, which have the ability to control adaptively various flow conditions, to time-varying flow fields have never been reported. In this chapter, an active separation control feedback system is developed in utilizing the results of earlier chapters and is practically applied to flow separation control of a diffuser.

8.1 Experimental Method

Experiments were conducted in a low speed wind tunnel. A schematic diagram of the wind tunnel is shown in Fig. 3.1. The test section had the function of a variable diffuser which could adjust the divergence angle between 0 and 45 degrees. In the present experimental system, flow does not separate at the divergence angle between 0 and 10 degrees. A detailed diagram of the test section is shown in Fig. 3.2. Jet flow was delivered through a metering valve after accumulating the air to a tank by using a compressor. A rotameter was placed downstream of the metering valve. Three jet orifices were placed at the upstream of the divergent lower wall and they were configured on the right-hand side of the lower wall in the test section (see Fig. 3.3). The jets were skewed at 90 degrees (θ =90 degrees) with respect to the freestream direction (0 degree being

downstream). If we do not mention particularly, we set the divergence angle of the test section, the jet pitch angle and the jet orifice diameter as α =20 degrees, ϕ =45 degrees and D_j=3 mm, respectively.

Velocity measurements were carried out using an X-array hot wire probe. The hot wire probe was supported by a three-axis computer-controlled traverse unit. The active separation control feedback system was practically applied to time-varying flow fields. In this study, the flow conditions could be changed by varying the freestream velocity and the divergence angle of the test section. Separation control was made in reference to the static pressure at two measurement points, in the upstream of the divergent portion (X=-150 mm, unstalled region) and in the divergent portion (X=110 mm). Static pressure measurements were carried out at several stations in the downstream direction (see Fig. 3.13) using a differential pressure transducer which had the ability to measure very small differential pressure (0.01 mmAq). The pressure value was converted from the output voltage of the differential pressure transducer. For the vortex generator jet method the strength of longitudinal vortices could be adjusted by varying the jet speed and therefore separation control corresponding to the degree of separation became possible by adjusting the jet speed. Figure 8.1 shows the flow chart of this system (Active Separation Control System Using Vortex Generator Jets: ASCSVGJ) and Fig. 8.2 shows the schematic diagram. This system mainly consists of a differential pressure transducer, a valve with controller, and a personal computer. The valve was actuated by an electric signal from the personal computer. In this system, a differential pressure between two points, the upstream of divergent portion and the measurement station in the diffuser, which judge the initial flow situation were measured initially. If a flow separation was detected, the vortex generator jet device operates and controls the jet speed to suppress the separation.

8.2 Results and Discussion

8.2.1 Control System of ASCSVGJ

The variable *dif* denotes the state value of this system for judging the flow situation, defined by

$$dif = \frac{dpv - dpv_{int}}{dpv_{uf} - dpv_{int}} \quad , \tag{8.1}$$

where *dpv* is the output voltage of the differential pressure transducer and the subscript *int* indicates the initial voltage when no wind blows and *uf* indicates the situation before issuing jets. A control reference *SV*, which was used as a judging parameter of the suppression of flow separation, was determined by using a state value of this system *dif*. Concretely speaking, *SV* is the state value of the system when the suppression of flow separation is achieved. Whether separation occurs or not is judged in reference to the flow visualization results. Therefore, if the system achieves the pressure recovery sufficiently above the control reference, the system judges the attainment of the control. Figure 8.3 shows the pressure recovery of the diffuser along the flow direction for two cases of control reference. For the case of SV-Case 1 the value of *SV* was set to 0.7. SV-Case 1 is provided for the purpose of attaining the suppression at X = 110 mm. For SV-Case 2 the value of *SV* was determined to maintain the suppression effect even in the further downstream. For both cases this system measures the static pressure at the same position in a diffuser (X=110 mm). It can be seen from Fig. 8.3 that at X=250 mm SV-case 2 has a more effective pressure recovery in comparison with SV-Case 1. In other words, this system has the ability to select basic (suppression up to the measurement position) and extended (suppression persisting further downstream) control by setting up the control reference *SV*. In this paper, SV-Case 1 is reported.

Figure 8.4 shows the differential pressure variation after this system began to suppress flow separation in three freestream velocities. Figure 8.4 indicates that effective pressure recovery can be achieved by

operating the system for each freestream velocity. This system continues to control after attaining the suppression of flow separation. In the control process, varying the freestream velocity causes change in the differential pressure. However, this system has the ability to correct the differential pressure change by including dpv_{uf} in the state value *dif*. In other words, this system enables us to judge the suppression effect using the same *SV* for different freestreams. In order to approach the state value *dif* to control reference *SV*, the jet speed is adjusted. The control variable q is defined as the jet flow rate per control step and is set to be constant. However, only for the situation in which *dif* approaches *SV*, the value of q is decreased and the overshooting of the target value is prevented.

8.2.2 Control Effect of ASCSVGJ

Figure 8.5 shows the flow visualization in the divergent portion of the test section for U_0=6.5 m/s. The surface tuft method was used as a diagnostic technique to observe the effect of the active separation control system on separated flows. Tufts were put on the lower wall of the test section at Z=140 mm. In Fig. 8.5, the air flows from left to right and the tuft of the downstream side of this figure is at X=110 mm. It is seen that this control system can suppress flow separation.

If the rate of pressure recovery of the diffuser is defined near the center axis of the wind tunnel, pressure losses may be neglected. Then from Eq. (2.10), the local pressure recovery coefficient C_{pL} for U_i and U_e is given by

$$C_{p_L} = \Delta p / \frac{1}{2}\rho U_i^2 \quad ; \quad \Delta p \approx \frac{1}{2}\rho(U_i^2 - U_e^2) \tag{8.2}$$

where subscript i and e indicate the inlet and outlet of the diffuser, respectively. In this study, U_i was measured at X=-10 mm and U_e at X=250 mm. Those two measurement stations are the movable limits of the traverse unit. For the case of U_0=6.5, 8.5 and 11.1 m/s, diffuser effectiveness ($\eta = C_{pL}/C_{pth}$) was 0.6, 0.5, and 0.4, respectively. The diffuser effectiveness for U_0=11.1 m/s was lower than that for the

other cases, because the effective suppression of flow separation was not achieved over a longer streamwise distance. For the same *VR* the vorticity of the longitudinal vortex became stronger as the freestream velocity became faster. The suppression of flow separation was achieved with low *VR* at X=110 mm for U_0=11.1 m/s in comparison with the other cases of U_0=6.5 and 8.5 m/s. Therefore, for U_0=11.1 m/s the suppression is not maintained in the downstream direction. From Fig. 8.3, it is clear that the effective pressure recovery in the downstream of X=200 mm is not achieved for SV-Case 1.

Using an X-array hot wire probe, we tried to measure the back-flow behavior in order to clarify the effectiveness of this system in separation control. The measurements were carried out by applying the manner shown by Nishi et al. [20]. As shown in Fig. 8.6, an X-array hot wire probe with an L-type support was inserted in the divergent portion of the test section so as to be perpendicular to the freestream direction. The increment of output of channel 2 is greater than that of channel 1 due to the blocked effect of the longer prong, if the flow is in the forward or downstream direction. On the other hand, under the back-flow condition the increment of output of channel 1 becomes greater than that of channel 2 because the longer prong does not affect the output. Making use of this character of X-array hot wire probe, the comparison of back-flow behavior between the cases in control and without control of this system was made. The output of X-array hot wire probe is shown in Fig. 8.7. It is seen that the output of the channel 1 decreases considerably in control and that of the channel 2 increases in control. Therefore, it can be said that the flow in the downstream direction increases for the case in control.

8.2.3 Applications of ASCSVGJ to the Separated Flow

In order to adaptively suppress flow separation, this system was

applied to time-varying flow fields caused by change in the freestream velocity or that of the divergence angle of the test section. Figures 8.8 and 8.9 show the time variation of differential pressure under control for the flow field which causes flow separation. In these figures, point "A" is just when the separation control is attained by operating the system. Point "B" indicates the point at which the flow condition is changed and point "C" is when the system senses change in the flow conditions and restarts to suppress the flow separation.

Figure 8.8(a) shows the differential pressure plotted against the control time for the situation in which flow separation occurs due to change in the freestream velocity after the suppression of flow separation has been attained. In this example, the flow is separated initially. The system tries to suppress flow separation and attains suppression at point "A". Beyond point "A", the system keeps the jet speed constant. When the freestream velocity is changed at point "B", the flow separation can not be suppressed by the given jet speed and therefore the differential pressure decreases. The system restarts to suppress flow separation at point "C" and as a result the suppression is attained at point "A". After that time, the system keeps the jet speed constant.

Figure 8.8(b) shows the time variation of the differential pressure for the situation in which no flow separation occurs, though the freestream velocity changes. The system initially tries to suppress flow separation for the separated flow field and attains the suppression at point "A". Beyond point "A", the system maintains constant jet speed. The freestream velocity changes at point "B", but the flow does not separate and the differential pressure increases. The system restarts at point "C" and decreases the jet speed. The differential pressure begins to decrease, and beyond point "A" the system keeps the jet speed constant. The system can decrease the jet speed in order to optimize performance or to avoid secondary air loss for issuing jets.

Figure 8.9(a) shows the case in which flow separation occurs due to change in the divergence angle of the test section. In this case, the flow is not separated initially because the divergence angle is small (α =10 degrees). The system senses to be unstalled and cuts off the jets

completely at point "A". Separation is suppressed without jet flow issuing (jet-off situation) at point "A". Flow separation is caused by change in the divergence angle of the test section at point "B". The system restarts to suppress the separation at point "C" and suppresses it. The system keeps the jet speed constant beyond point "A".

Figure 8.9(b) shows the case in which no flow separation occurs even with change in the divergence angle. The system maintains the jet speed after suppression of the flow separation is once attained at point "A". When the divergence angle is changed at point "B", the flow condition indicates the unstalled flow field. Therefore, the system restarts to optimize the performance at point "C" and finally attains the optimal condition at point "A", which is in the jet-off situation.

8.2.4 Control Time of ASCSVGJ

The control time which is necessary to attain separation control is related to the response speed against the change of flow field. In other words, the more quickly flow situations are responsible to the system, the faster separation control can be performed. For the case of the jet pitch angle of 30 degrees, time variation of differential pressure under control is shown in Fig. 8.10. Comparing the 30-deg case with the 45-deg case (see Fig. 8.4), the 30-deg case attains the control target more rapidly than that for the 45-deg case among the three cases of freestream velocity. Figure 8.11 indicates the mean vorticity distribution over the spanwise direction at X=110 mm. For the 30-deg case, the vorticity is stronger and the vortices are lower in comparison with the 45-deg case. Therefore, the case of a pitch angle of 30 degrees makes effective the pressure recovery and also the suppression of flow separation at X=110 mm, where the differential pressure is measured (*cf.* Chapter 7). This result means that the system could attain the control quickly, if the difference between the differential pressures of stalled and unstalled flow fields is large. In other words, the system can be operated stably and controlled more quickly, if

pressure fluctuations can be neglected in comparison with a large pressure recovery.

In these experiments, the jet flow rate per control step is kept constant for various flow situations. However, if the jet flow rate is variable in attaining the control target, a faster response system can be developed. In the next section, we will explain the improved system (Improved ASCSVGJ: IASCSVGJ) which is the faster response system compared with the original system.

8.2.5 Improved ASCSVGJ by Considering Control Time

In order to attain a faster response, ASCSVGJ is improved. The alteration points from ASCSVGJ to IACSCVGJ are that 1) the jet pitch angle is set at 30 degrees in order to make effective the pressure recovery and also the separation control at X=110 mm, where the differential pressure are measured (*cf.* Chapter 7), 2) the jet flow rate per control step varies adaptively for various flow situations, and 3) the jet orifice is 2 mm in diameter. The alteration point 1) or 2) is useful to decrease the number of sampling data and the control step because pressure fluctuations in the system can be reduced by a large pressure recovery and therefore the system attains a faster response. The alteration point 3) is used for the purpose of avoiding secondary air loss for issuing jets. For the D_f=3 and 2 mm cases the comparison between the streamwise vorticity contours is shown in Fig. 8.12. Comparing the case of D_f=3 mm with that of D_f=2 mm, we see that the D_f=3 mm case gives broad longitudinal vortices in the spanwise direction because jet orifices become wider in the spanwise direction due to the jet pitch angle. This means that the controlled region is spread in the spanwise direction and make more effective separation control in comparison with the D_f=2 mm case. Therefore, the D_f=3 mm case gives small VR for the control target. However, the D_f=3 mm case

gives lager jet flow rate than the D_j=2 mm case. For example, the jet flow rate and VR are Q_j=25 l/min and VR=7, respectively, for D_j=2 mm and ϕ =30 degrees (corresponding to the improved system). In addition, the jet flow rate and VR are Q_j=48 l/min and VR=6, respectively, for D_j=3 mm and ϕ =45 degrees (corresponding to the original system). Table 8.1 gives the values of the jet flow rate and VR for three different freestream velocities when the system attains the control. The D_j=2 mm case for a pitch angle of 30 degrees can avoid the jet flow loss because the jet flow rate is the only control variable in this system.

For the improved system time variation of differential pressure under control is shown in Fig. 8.13. Comparing Fig. 8.13 with Fig. 8.4, it is seen that the control time of the improved system is shorter than that of the original system for each freestream velocity.

Figures 8.14 and 8.15 show the time variation of differential pressure under control for time-varying flow fields caused by change in the freestream velocity and the divergence angle of the test section. Points "A", "B", and "C" in these figures indicate the same meaning as those in Fig. 8.8 or 8.9. Figure 8.14 shows the differential pressure plotted against the control time for the situation in which flow separation occurs due to change in the divergence angle of the test section for each freestream velocity. Figure 8.15 shows the case in which flow separation occurs due to change in the divergence angle and the freestream velocity. We can see from Fig. 8.14 or 8.15 that this improved system can adapt flow situation continuously and can achieve faster separation control in comparison with the original system.

8.3 Conclusions

An active separation control system using vortex generator jets which can adapt to various flow conditions was developed. We conclude that our active separation control system can adaptively suppress flow separation for flow fields caused by some changes in

freestream velocity and the divergence angle of the test section. Furthermore, for the control time which is important in the design of actual system, data for developing the system with a quick response were obtained.

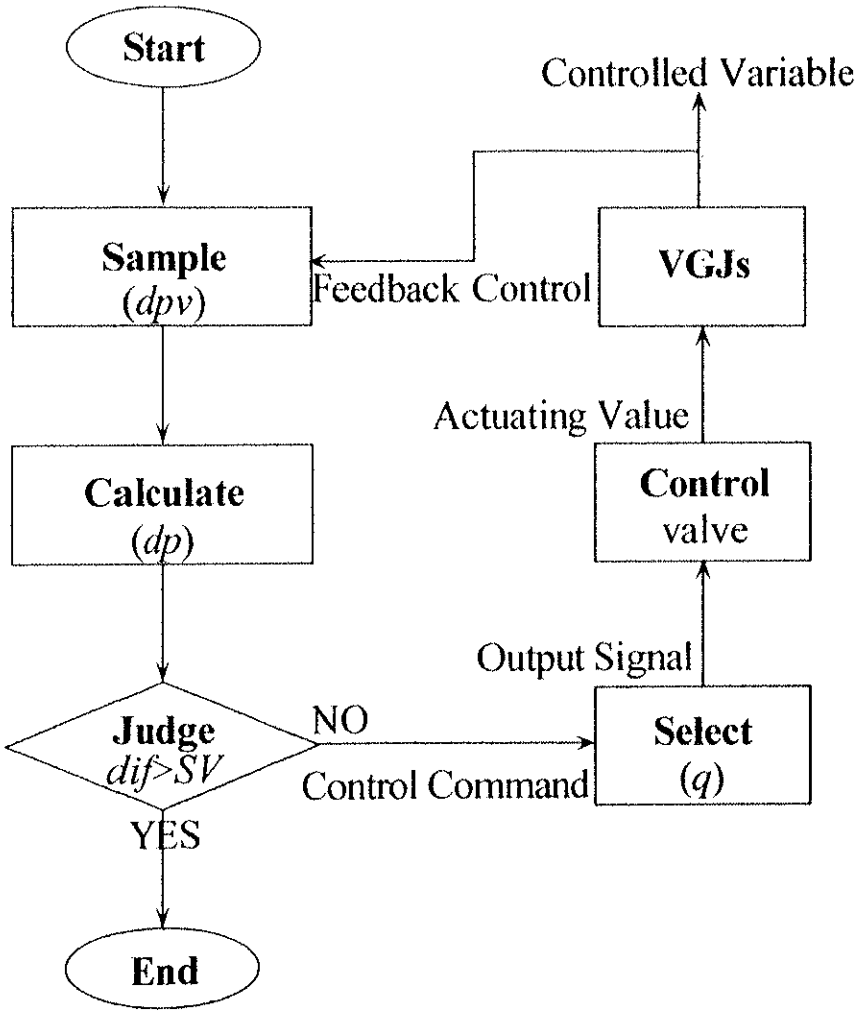

Figure 8.1 Flow chart of ASCSVGJ.

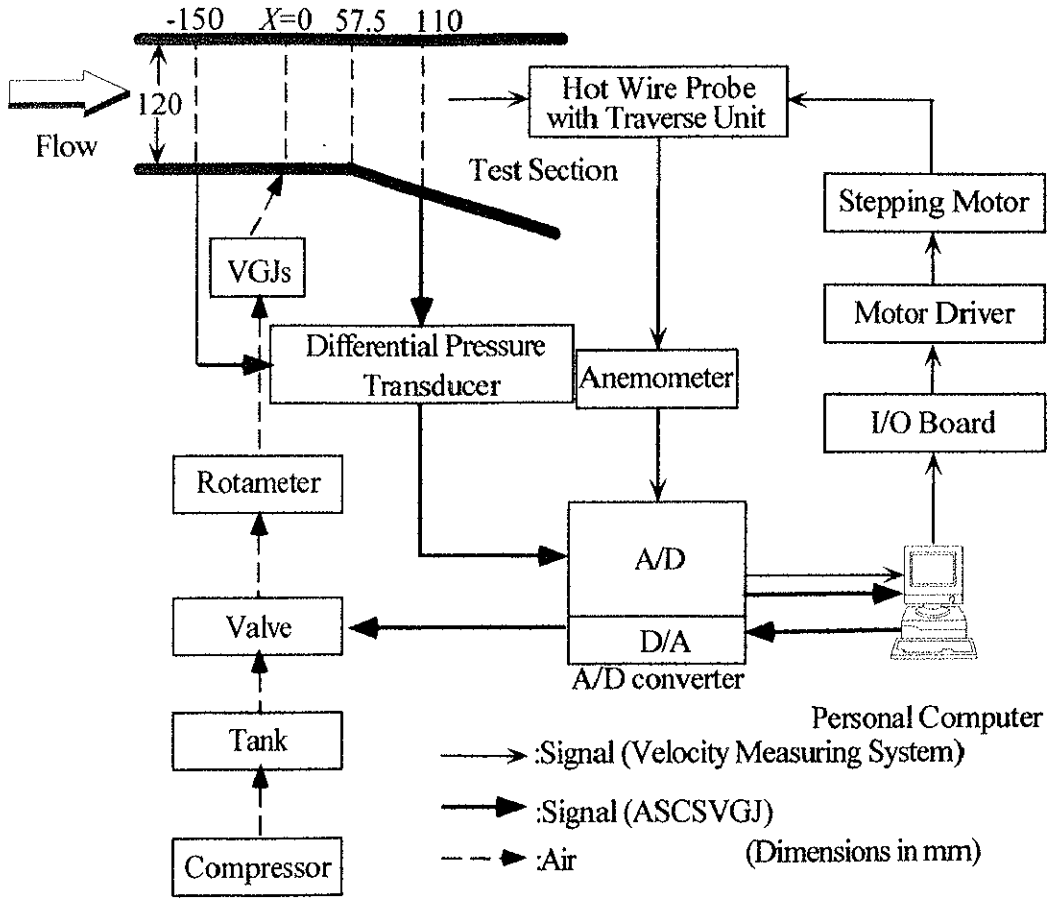

Figure 8.2 Schematic diagram of ASCSVGJ.

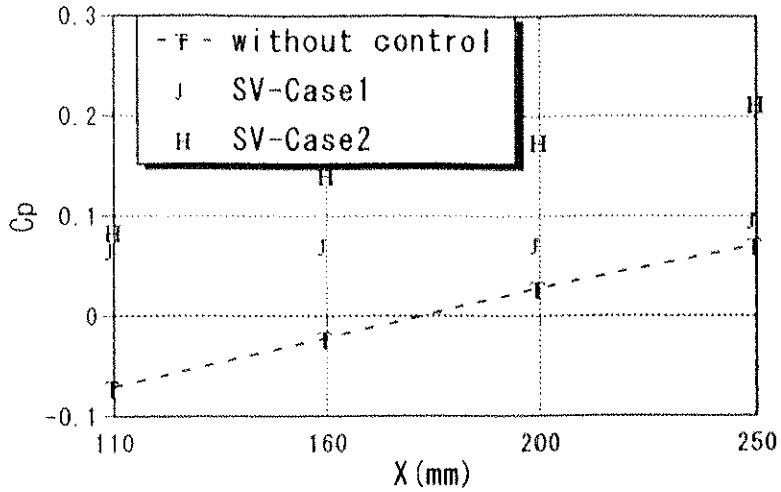

(a) U_0=6.5 m/s

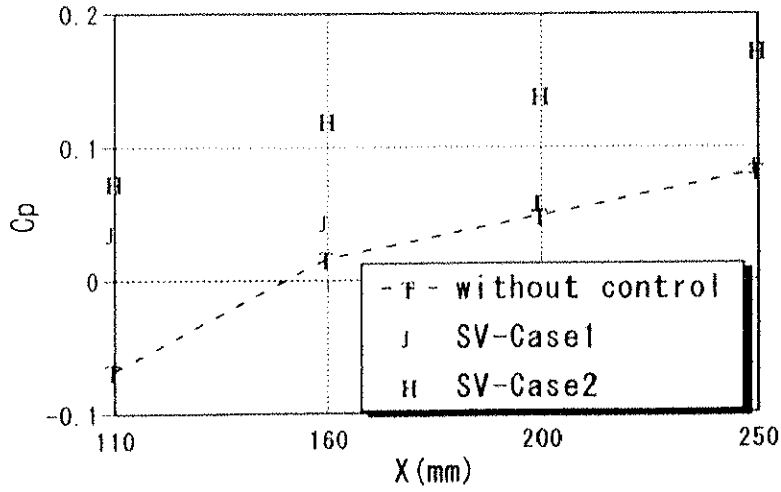

(b) U_0=8.5 m/s

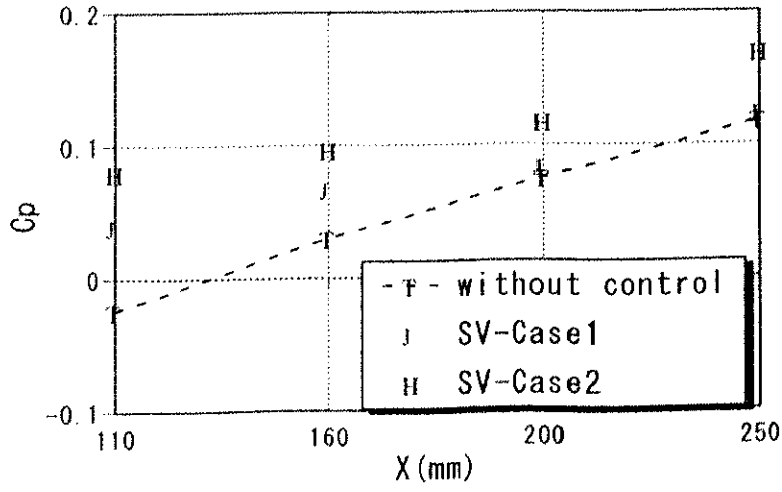

(c) U_0=11.1 m/s

Figure 8.3 Pressure distribution in the downstream direction.

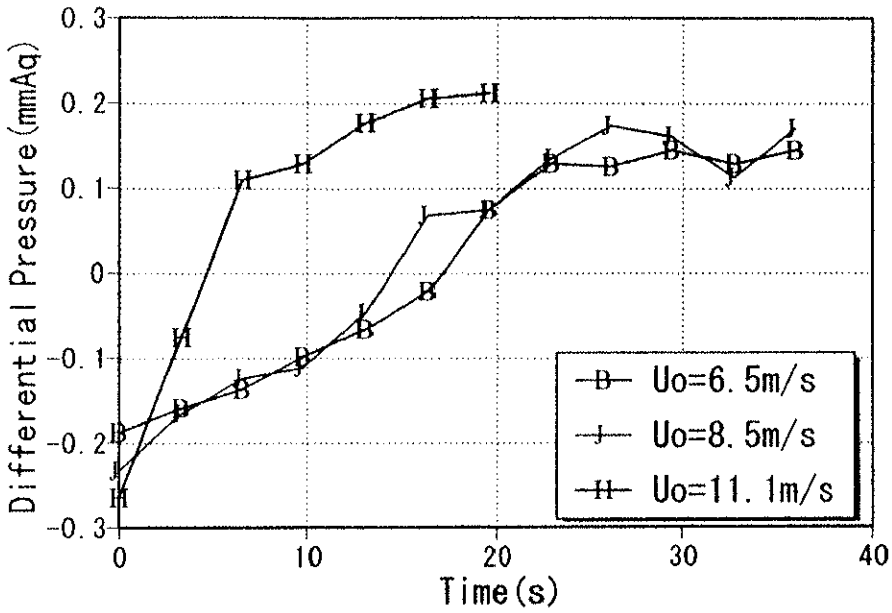

Figure 8.4 Variation of differential pressure under control.

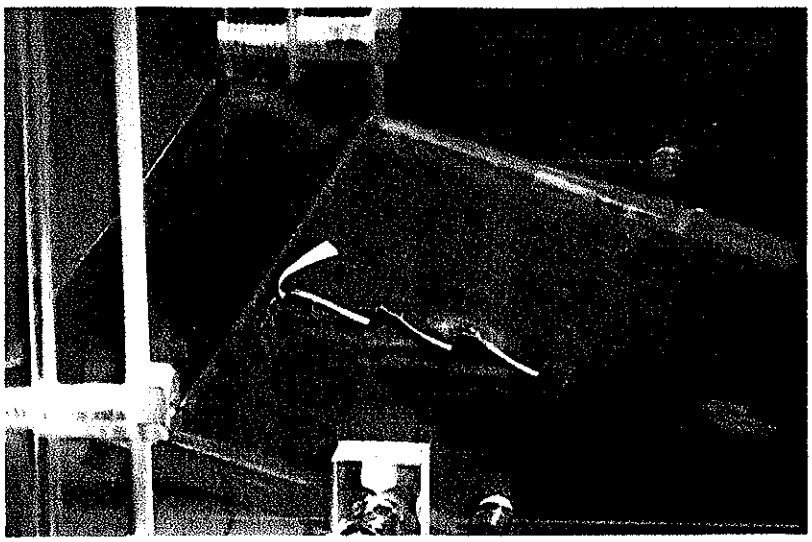

(a) Without control

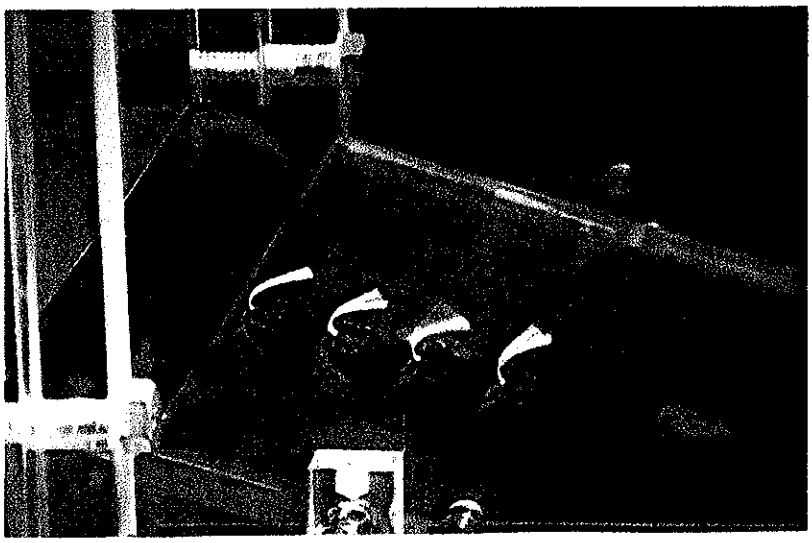

(b) With control

Figure 8.5 Surface flow in divergent portion of the test section (U_0=6.5 m/s).

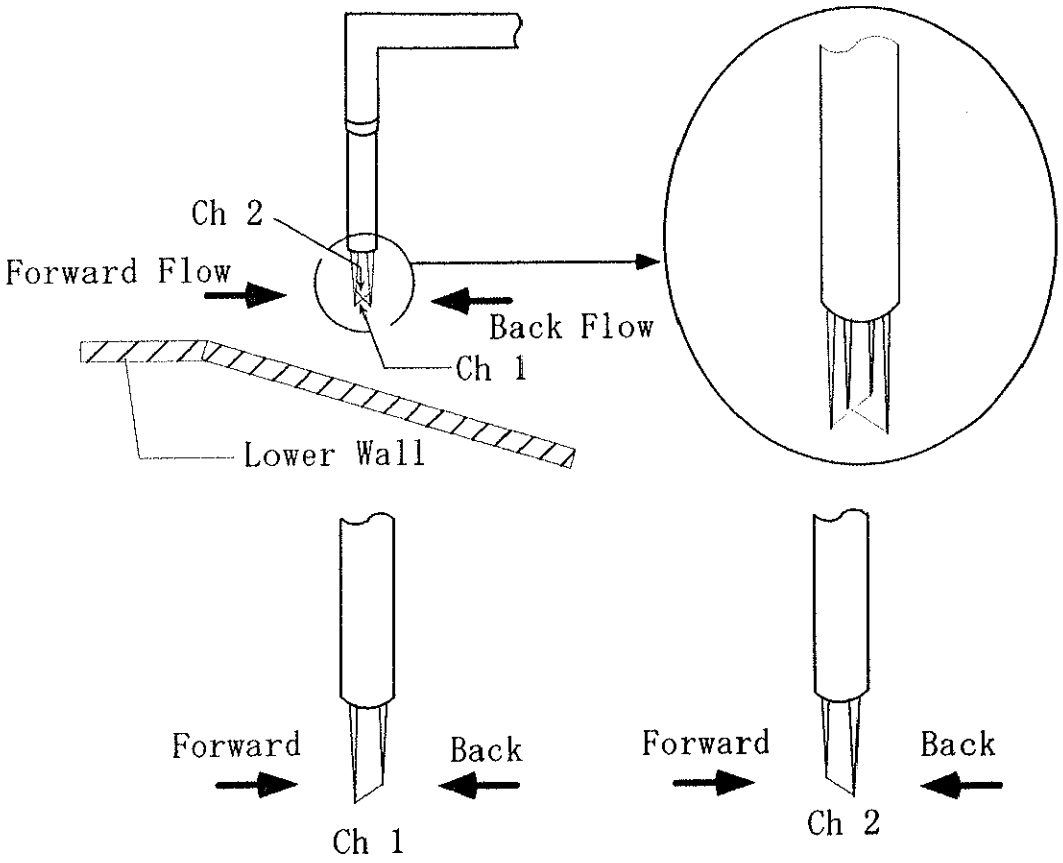

Figure 8.6 Channel 1 or 2 position of X-array hot wire probe.

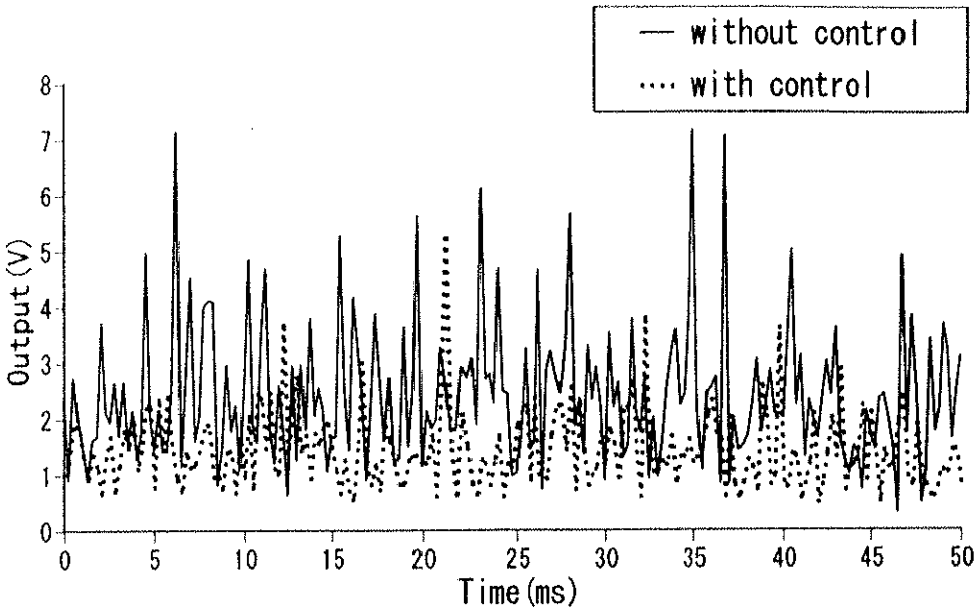

(a) Channel 1 output

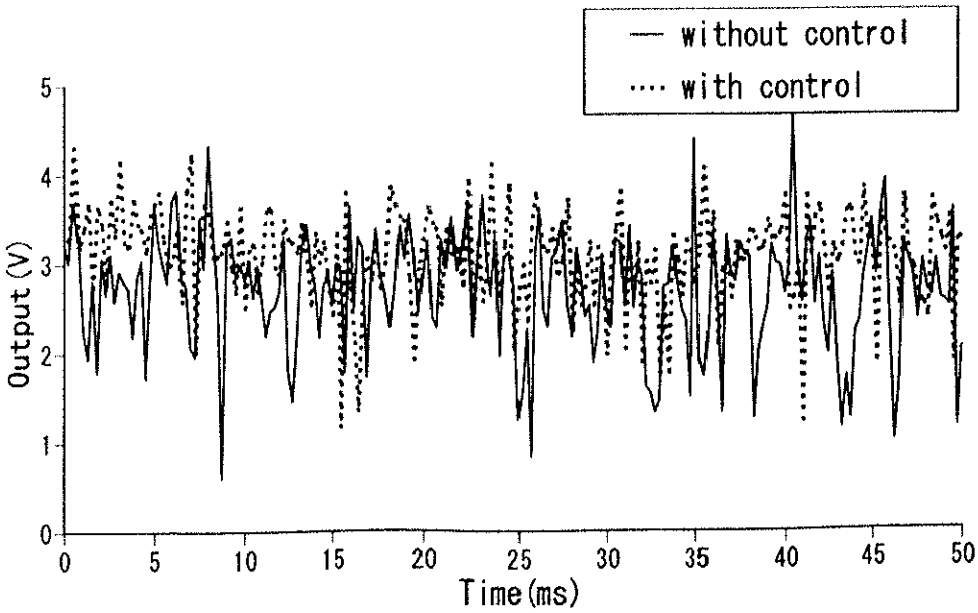

(b) Channel 2 output

Figure 8.7 Output of velocity signals at X=110 mm, Y=-4 mm, Z=160 mm (U_0=6.5 m/s).

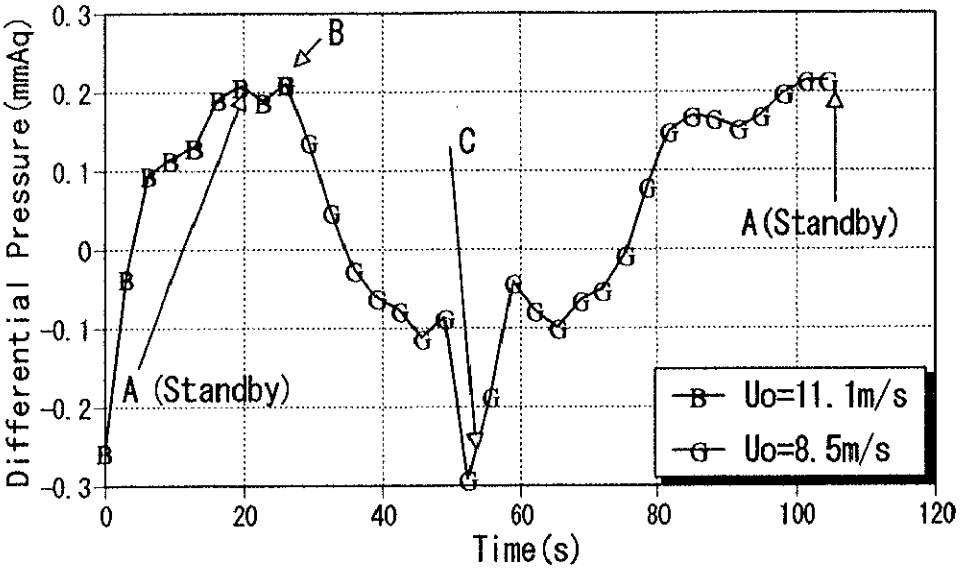

(a) U_0=11.1 m/s → 8.5 m/s

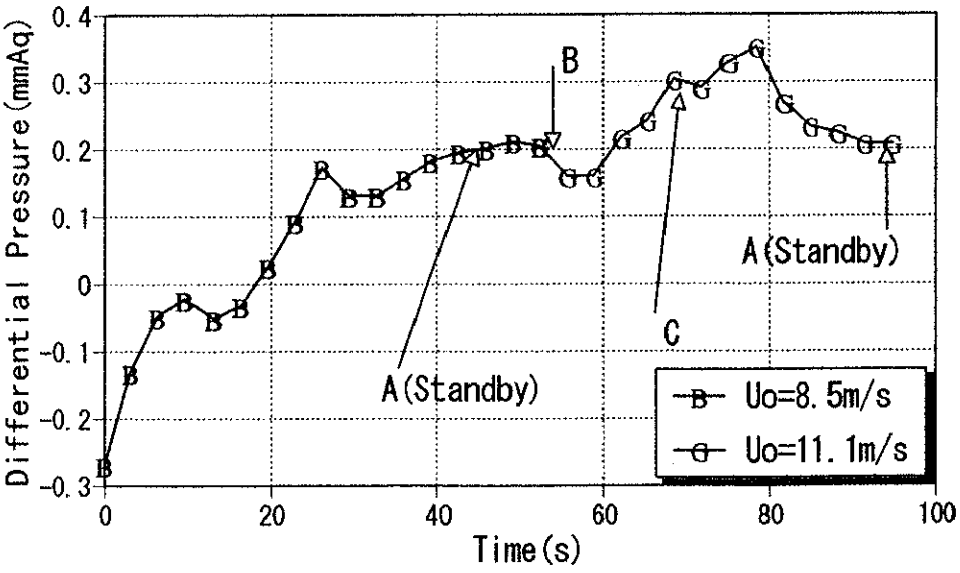

(b) U_0=8.5 m/s → 11.1 m/s

Figure 8.8 Variation of differential pressure under control.

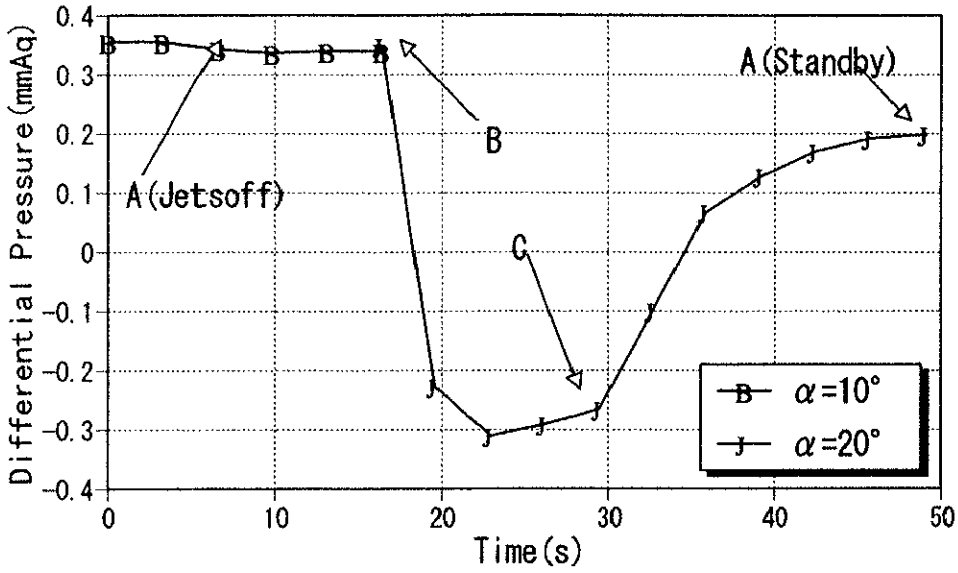

(a) α =10 deg → 20 deg

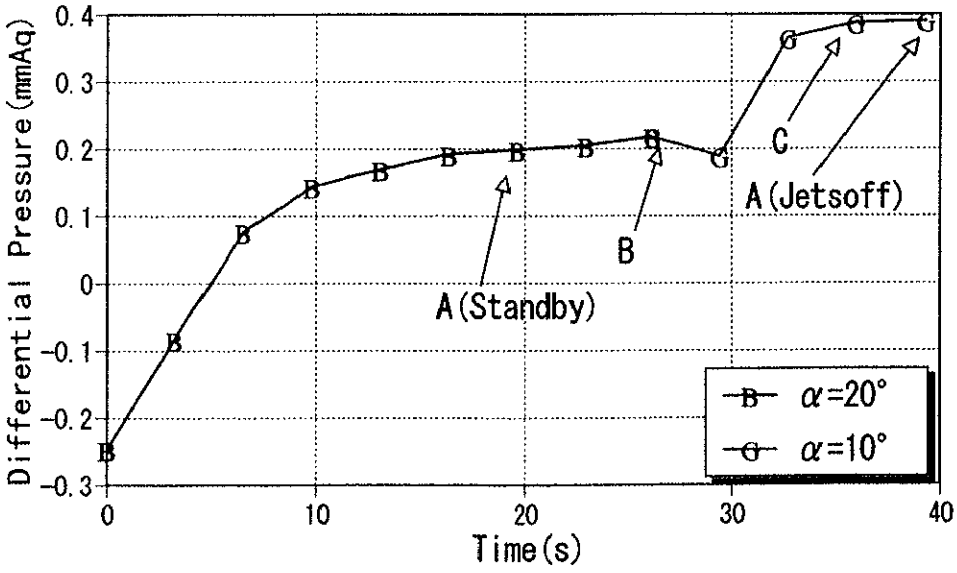

(b) α =20 deg → 10 deg

Figure 8.9 Variation of differential pressure under control (U_0=11.1 m/s).

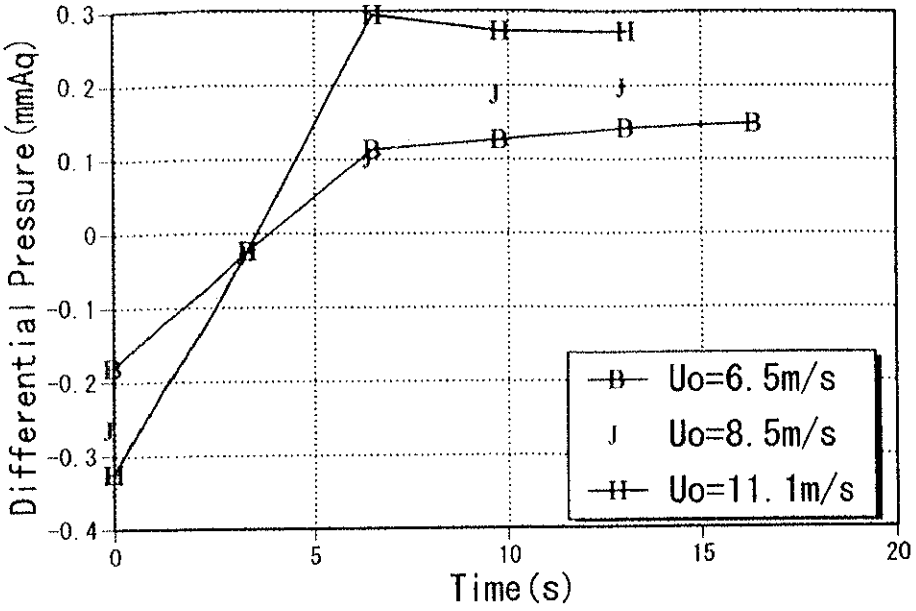

Figure 8.10 Variation of differential pressure under control (ϕ =30 deg, D_f=2 mm).

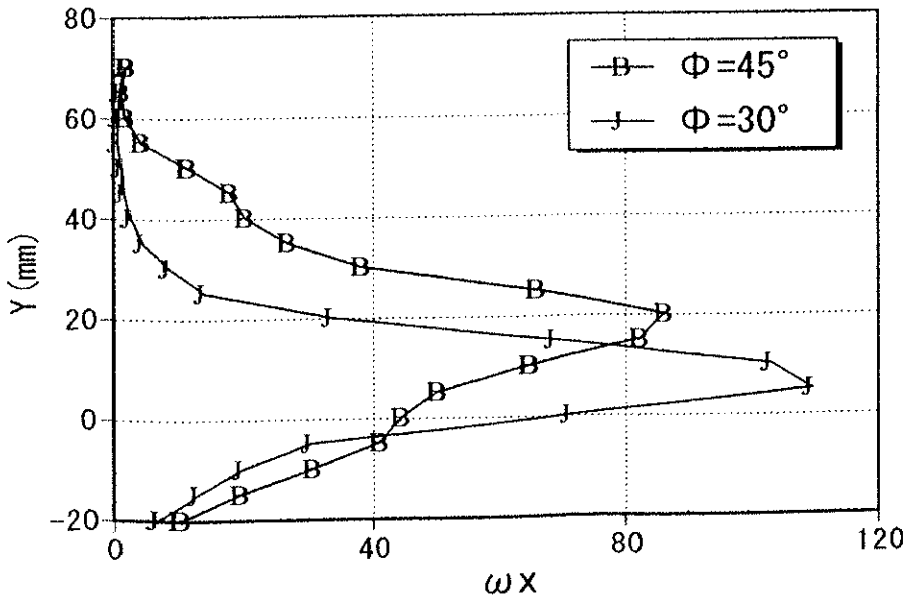

Figure 8.11 Mean vorticity in spanwise direction at X=110 mm (U_0=6.5 m/s, VR=9.5, D_f=2 mm).

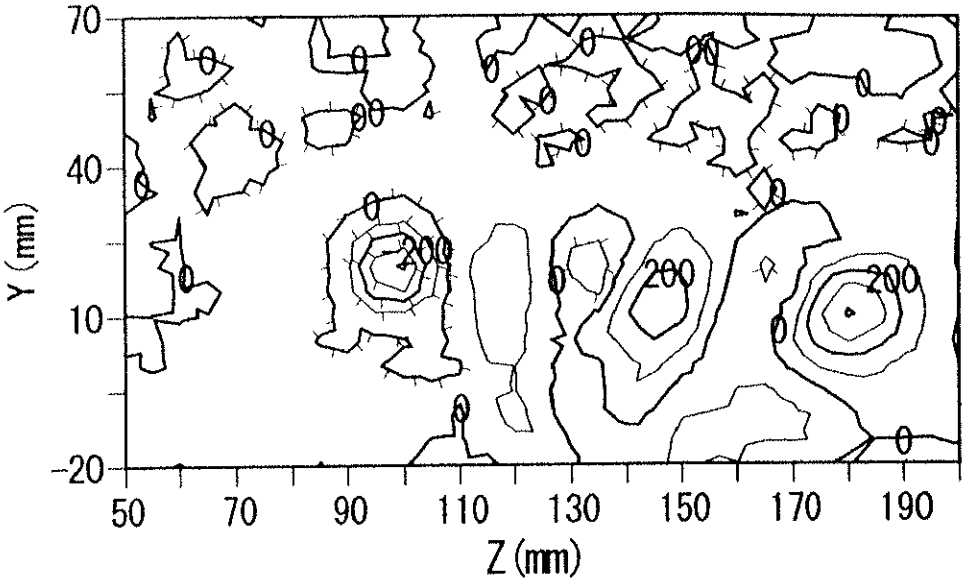

(a) D_f=2 mm

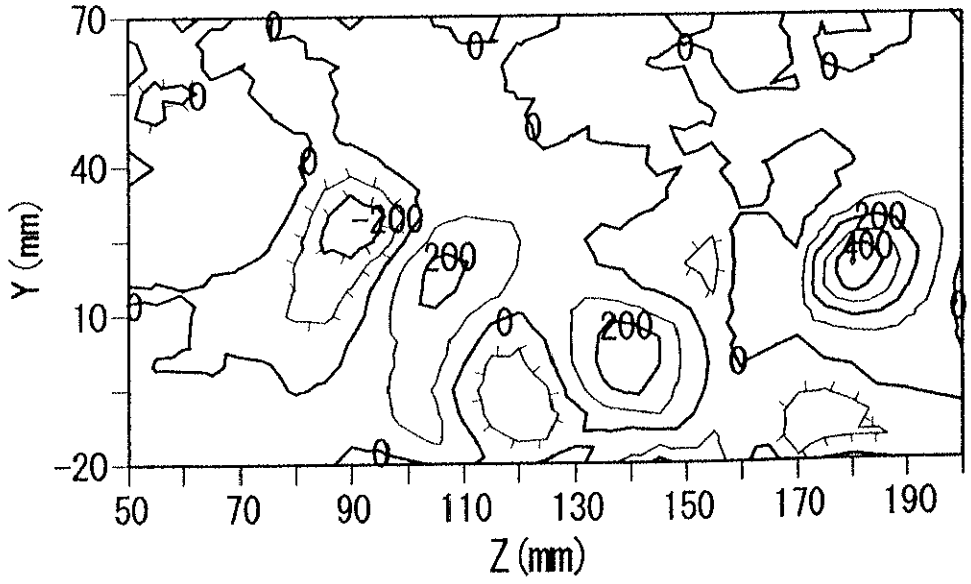

(b) D_f=3 mm

Figure 8.12 Contours of streamwise vorticity at X=110 mm (U_0=6.5 m/s, VR=9.5). Decorated lines denote negative vorticity. Contour interval=100 1/s.

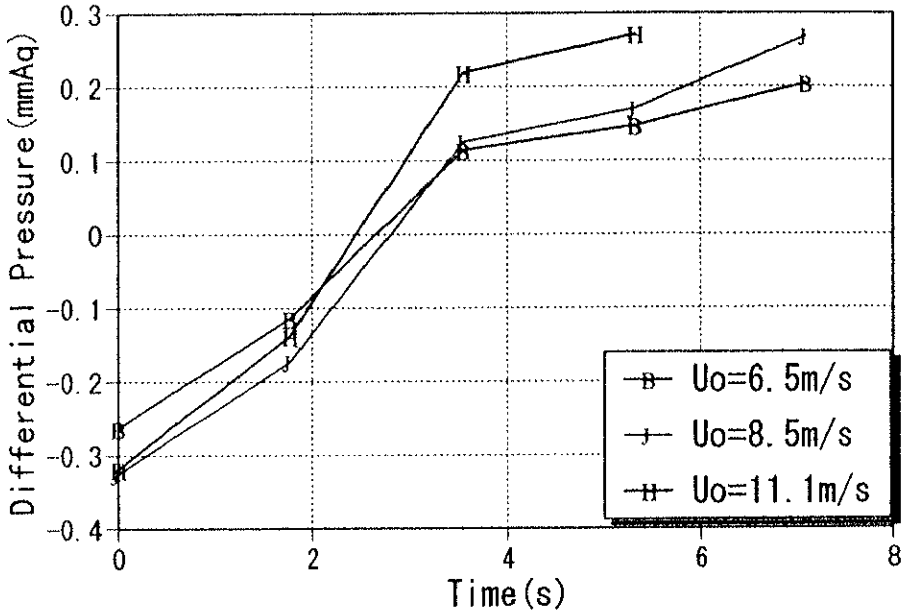

Figure 8.13 Variation of differential pressure under control with IASCSVGJ.

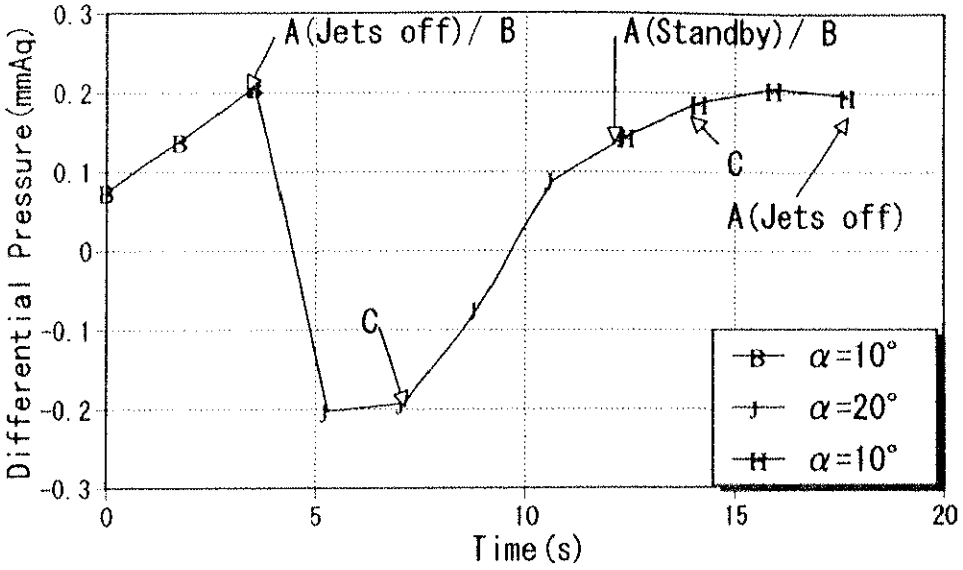

(a) α =10 deg → 20 deg → 10 deg (U_0=6.5 m/s)

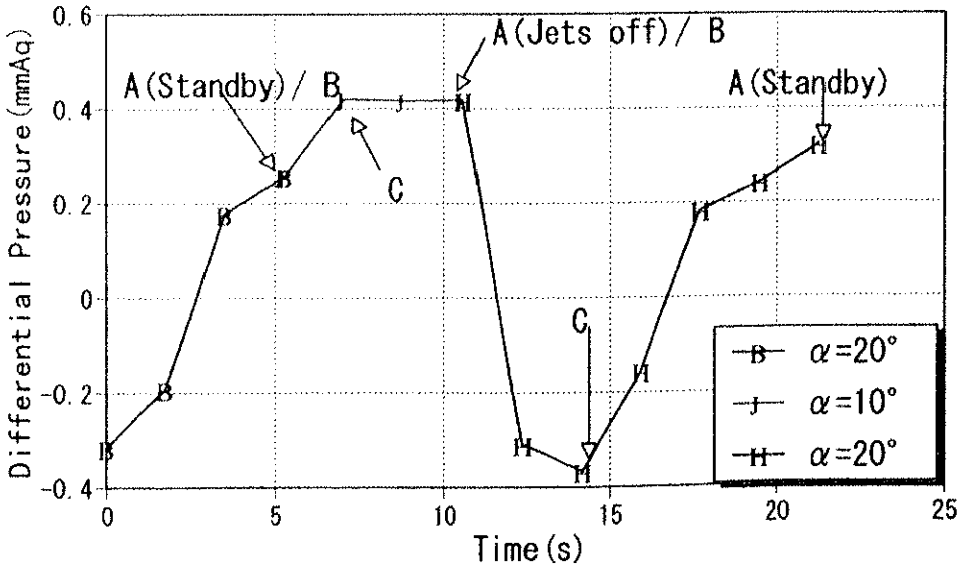

(b) α =20 deg → 10 deg → 20 deg (U_0=11.1 m/s)

Figure 8.14 Variation of differential pressure under control with IASCSVGJ.

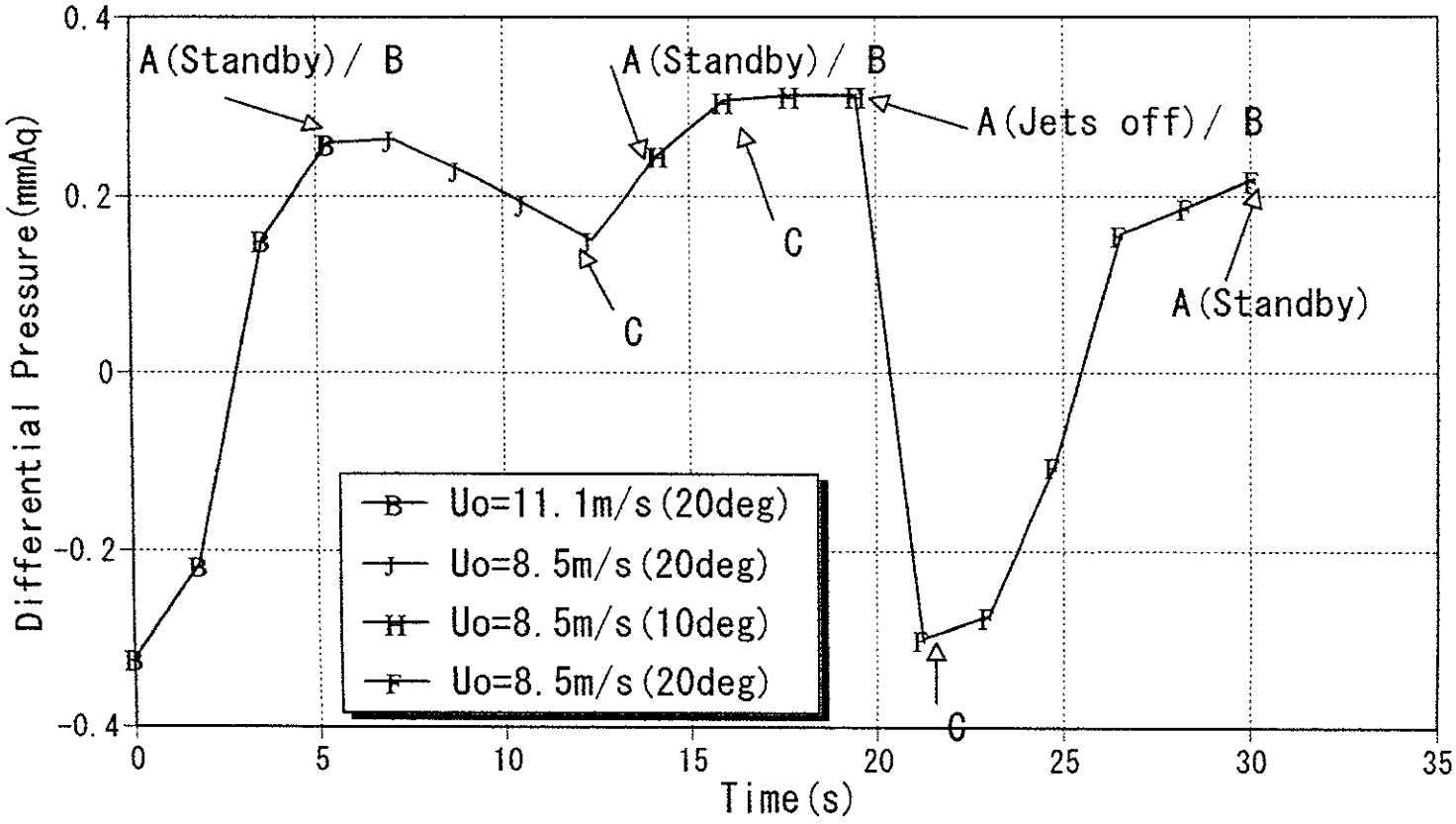

Figure 8.15 Variation of differential pressure under control with IASCSVGJ.

Table 8.1 Values of jet flow rate and VR when the system attains control

Jet Orifice Diameter D_j (mm)	Pitch Angle ϕ (degree)	Freestream Velocity U_0 (m/s)	Jet Flow Rate Q_j (l/min)	VR
2	30	6.5	25	7
3	45	6.5	48	6
2	30	8.5	29	6
3	45	8.5	45	4
2	30	11.1	21	3
3	45	11.1	28	2